Journal of Vacuum Science & Technology A

Deposition of polycrystalline Si and SiGe by ultra-high vacuum chemical molecular epitaxy

K. M. Chen, H. J. Huang, C. Y. Chang, L. P. Chen, and G. W. Huang

Citation: Journal of Vacuum Science & Technology A **18**, 1196 (2000); doi: 10.1116/1.582324
View online: http://dx.doi.org/10.1116/1.582324
View Table of Contents: http://scitation.aip.org/content/avs/journal/jvsta/18/4?ver=pdfcov
Published by the AVS: Science & Technology of Materials, Interfaces, and Processing

---

Deposition of polycrystalline Si and SiGe by ultra-high vacuum chemical molecular epitaxy

K. M. Chen,[a] H. J. Huang, and C. Y. Chang
Department of Electronics Engineering and Institute of Electronics, National Chiao-Tung University, Hsin-Chu, Taiwan 300 Republic of China

L. P. Chen and G. W. Huang
National Nano Device Laboratory, Hsin-Chu, Taiwan 300 Republic of China

(Received 20 August 1999; accepted 7 February 2000)

The polycrystalline $Si_{1-x}Ge_x$ (poly-$Si_{1-x}Ge_x$) films have better properties than poly-Si for device fabrications, such as lower proceeding temperature and process thermal budget. For these reasons, the poly-$Si_{1-x}Ge_x$ films have been utilized for low-temperature thin film transistor fabrications and gate electrodes of metal–oxide–semiconductor transistors. In this work, disilane and germane were used to grow poly-$Si_{1-x}Ge_x$ films at low temperature ($<600\,°C$) by the cold-wall type ultrahigh vacuum chemical molecular epitaxy system. The poly-$Si_{1-x}Ge_x$ films were deposited on oxide and nitride surfaces. The Ge fraction x was evaluated from x-ray diffraction and Auger electron spectroscopy. It is observed that the Ge fraction increases with the increase of the GeH_4 flow rate. The result is only slightly related to the substrate type. The growth rate increases with the Ge fraction at lower values and then decreases with the Ge fraction in the higher composition range. This implies that the growth mechanism of poly-$Si_{1-x}Ge_x$ films is different from that of epitaxial $Si_{1-x}Ge_x$ on Si. The uniformity of poly-$Si_{1-x}Ge_x$ films depends on the Ge fraction, and it is improved by the addition of germanium. The result can be explained by the lower activation energy (<0.25 eV) of poly-$Si_{1-x}Ge_x$ deposition as compared to that of poly-Si (~ 2.1 eV). From the x-ray diffraction and atomic force microscopy analyses, the crystallinity and surface roughness of films are suitable for device fabrications. © *2000 American Vacuum Society.* [S0734-2101(00)07704-6]

I. INTRODUCTION

Polycrystalline silicon–germanium (poly-$Si_{1-x}Ge_x$) has recently been shown to be a favorable alternative to polycrystalline silicon (poly-Si) for various applications in integrated circuit (IC) technologies.[1–5] Since the melting point of $Si_{1-x}Ge_x$ is lower than that of Si, the fabrication processes such as deposition, crystallization, and dopant activation occur at lower temperatures for $Si_{1-x}Ge_x$ than for Si. In addition, poly-$Si_{1-x}Ge_x$ films with Ge mole fractions up to 0.6 are compatible with mature Si technologies. Poly-$Si_{1-x}Ge_x$ films have been utilized for the low temperature thin film transistor (TFT) fabrications without exceeding 550 °C,[1] whereas comparable TFTs fabricated in poly-Si require proceeding temperatures at or above 600 °C. The significant reductions in process temperature afforded by poly-$Si_{1-x}Ge_x$ make it a promising material for TFT IC applications. Furthermore, with lower resistivity and variable work function, the heavily doped *p*-type poly-$Si_{1-x}Ge_x$ is an interesting gate-electrode material for submicrometer complimentary metal–oxide–semiconductor technologies.[2–5] The work function of P^+ poly-$Si_{1-x}Ge_x$ decreases with increasing Ge mole fraction x, so that the threshold voltage can be adjusted simply by varying the Ge content inside the films.[3] This allows one to reduce the surface channel doping while retaining the same threshold voltage as for poly-Si gate. This result increases the current drivability, the transconductance, and decreases the subthreshold swing of the transistor.[4] Since the higher dopant activation rate and lower diffusivity of boron atoms in poly-$Si_{1-x}Ge_x$ film are compared to poly-Si films, the boron penetration and poly-gate depletion effect can be reduced for poly-$Si_{1-x}Ge_x$ gated metal–oxide–semiconductor field effect transistors (MOSFETs).[5] Finally, poly-$Si_{1-x}Ge_x$ can be used as local interconnects when efficient activation of carriers with suppression of diffusion is required.

Among the published reports, poly-$Si_{1-x}Ge_x$ film can be formed by conventional low-pressure chemical vapor deposition (LPCVD),[6–9] the rapid thermal LPCVD,[10,11] and ultrahigh vacuum (UHV) CVD systems.[12,13] Deposition of poly-Si films at reduced pressures (<10 mTorr) has been investigated to achieve low temperature processing.[14–16] It has been found that the transition temperature for an as-deposited Si film from a polycrystalline to an amorphous state is dependent on the growth pressure, and is significantly lowered at reduced pressures.[14] In a previous report, the poly-$Si_{1-x}Ge_x$ with a fine grain structure has been demonstrated at temperatures as low as 500 °C using UHVCVD.[12–17] Therefore, UHVCVD shows the most promising method for low-temperature poly-Si film deposition.

In this article, the deposition of undoped poly-$Si_{1-x}Ge_x$ films onto SiO_2 and Si_3N_4 in a UHV chemical molecular epitaxy (UHVCME) system is described. This UHVCME system features a cold-wall reactor with an extremely low base pressure ($\sim 10^{-10}$ Torr) as well as the reduced deposition pressures (<1 mTorr). These conditions allow ex-

---

[a] Author to whom correspondence should be addressed; electronic mail: u8511801@cc.nctu.edu.tw

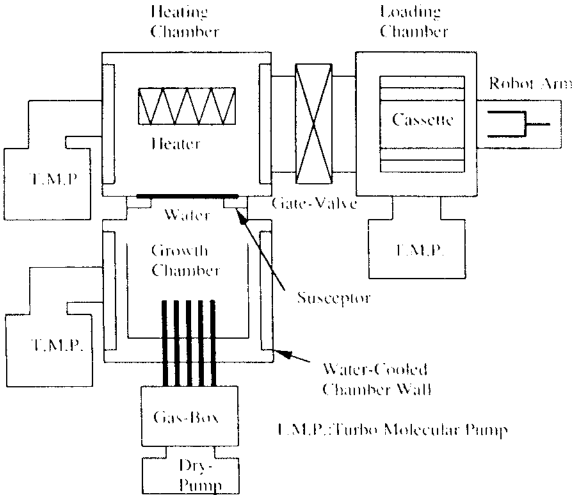

FIG. 1. Schematic diagram of the ultra-high vacuum chemical molecular epitaxy (UHVCME) system.

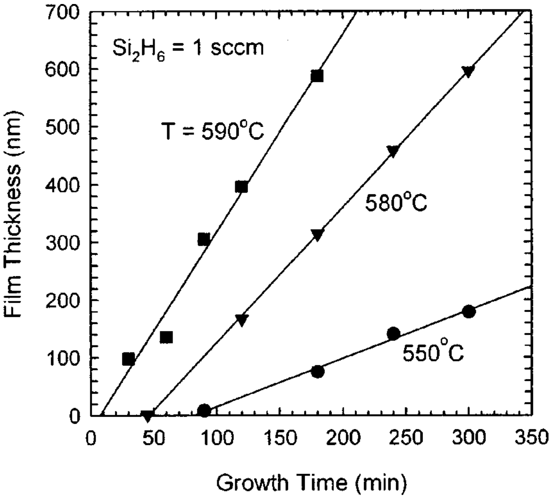

FIG. 2. Film thickness vs growth time for poly-Si grown on SiO_2 at different growth temperatures. The Si_2H_6 flow rate remained at 1 sccm.

tremely low temperature (below 550 °C) $Si/Si_{1-x}Ge_x$ epitaxial growth to proceed on the Si substrate.[18,19] The dependence of the Ge fraction and growth rate on the Si_2H_6 and GeH_4 flow rates are evaluated from x-ray diffraction (XRD) and surface profile measuring system, respectively. The growth mechanisms of poly-Si and poly-$Si_{1-x}Ge_x$ have been discussed and compared with that of epitaxial $Si/Si_{1-x}Ge_x$. The surface morphology and structure properties of these films are also presented.

II. EXPERIMENT

The UHVCME system used in this study includes a water-cooled cold wall stainless steel growth chamber, a loading chamber, separate nozzles for process gases, and a computer-controlled gas switching box. A schematic drawing of this system is shown in Fig. 1. The growth chamber is pumped by a 1000 ℓ/s turbomolecular pump and a base pressure of 2×10^{-10} Torr can be obtained. The chamber pressure is also maintained below 1×10^{-3} Torr during the deposition process by this pump. The wafers were loaded into the loading chamber and then the chamber was pumped down to 10^{-6} Torr as soon as possible. After the wafers were transferred into the growth chamber for deposition, the heater was lowered and started to heat the wafer to the deposition temperature at a ramp of 150 °C/min. Source gases are pure disilane from 1 to 10 sccm and pure germane from 1 to 10 sccm. The flow rates of reaction gases are controlled precisely by their own mass-flow controllers. In this work, 6 in. (100) Si wafers coated with a thermal oxide or nitride were used as the substrates. Prior to deposition, the substrates were cleaned using the standard RCA cleaning procedure. With this treatment, the wafers were subjected to a 5:1:0.25 $H_2O:H_2O_2:NH_4OH$ bath at 75 °C for 10 min, followed by a 10 min rinse in de-ionized (DI) water, and then to a 5:1:1 $H_2O:H_2O_2:HCl$ bath at 75 °C for 10 min, followed by a 10 min rinse in DI water and spin dry.

The thicknesses of the deposited films were determined by using a masked etch and measuring the step height using a surface profile measuring system with an accuracy within 20 nm. The Ge fraction of the deposited poly-$Si_{1-x}Ge_x$ films was primarily evaluated by XRD. To verify the accuracy of the XRD method, Auger electron spectroscopy (AES) was also performed to determine the Ge fraction with careful calibration. Atomic force microscopy was used to investigate the surface morphology of the deposited films.

III. RESULTS AND DISCUSSIONS

Figure 2 shows a typical plot of thickness measurement as a function of growth time for the poly-Si films deposition on SiO_2 at different temperatures. The slope of the fit line and its intercept with the x axis are defined as the growth rate and the incubation time, respectively, for each growth temperature. As illustrated, the poly-Si nucleation on an insulating substrate did not begin immediately, and there was an initial short period during which the poly-Si was not observed on insulating substrate by scanning electron microscopy (SEM). It is clearly noted that the growth rate increases while the incubation time decreases with increasing growth temperature. The increase of incubation time with decreasing growth temperature is due to slower nucleation and growth rates at lower temperatures.[17] Figure 3 shows the incubation time of poly-$Si_{1-x}Ge_x$ films grown at 550 °C for thermal oxide and nitride substrate as a function of the GeH_4 flow rate. With oxide substrate, a considerable amount of the incubation time is due to the rather low deposition rate (~0.9 nm/min) as well as the low generation rate of the nuclei.[17] Because of the long incubation time for SiO_2 substrate, we found that the poly-$Si_{1-x}Ge_x$ film cannot be directly deposited on the gate oxide for poly-$Si_{1-x}Ge_x$ gated MOSFET fabrication, and the gate oxide was destroyed under the UHV environment. To avoid this problem, a thin nitride layer must be deposited on gate oxide before the poly-$Si_{1-x}Ge_x$ growth. With a nitride substrate, the incubation time was about eight times smaller

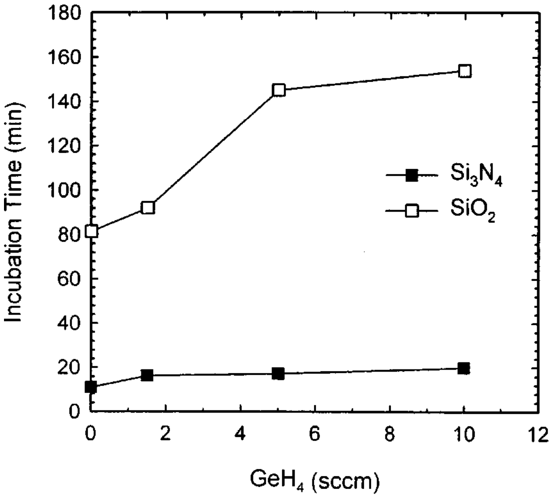

FIG. 3. Incubation time for poly-Si$_{1-x}$Ge$_x$ films deposited at 550 °C as a function of GeH$_4$ flow rate.

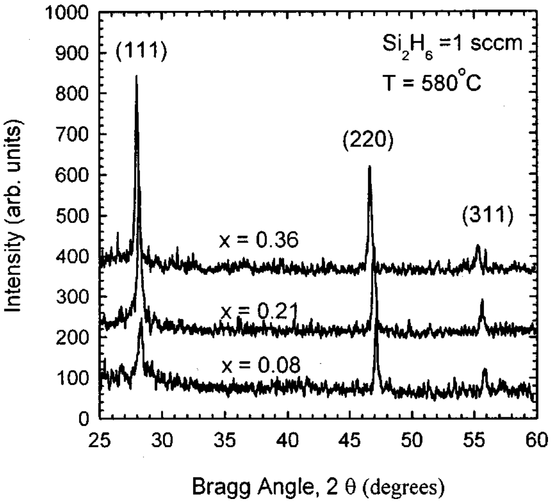

FIG. 5. X-ray diffraction data for 200 nm thick poly-Si$_{1-x}$Ge$_x$ films deposited at 580 °C.

than that of the oxide substrate. This fact suggests that, on a nitride surface, the generation rate of the nuclei is larger than that on an oxide surface. This may be due to either the higher areal density of chemical bonds on the nitride surface, or the chemical difference between oxide and nitride.[20] In both cases, we found that the addition of GeH$_4$ increases the incubation time. This result may be due to the higher surface mobility of Ge adatoms on the substrate surface which retard the generation of nuclei.

In this study, we found that the substrate type did not affect the Ge fraction and growth rate of the poly-Si$_{1-x}$Ge$_x$ films. Figure 4 is an Arrhenius plot of deposition rates versus reciprocal of the growth temperatures. The activation energy associated with pure poly-Si growth was found to be about 2.1 eV. This value is the same as the activation energy of Si epitaxy with the UHVCME system. The growth of poly-Si follows an identical mechanism of Si epitaxy on the (100) Si surface. The activation energy for the Si growth rate corresponds to the energy required for hydrogen atoms to desorb from the Si(100) surface.[21] This is evidence that the Si deposition rate is controlled by the desorption rate of hydrogen from the substrate surface. When GeH$_4$ was added, the poly-Si$_{1-x}$Ge$_x$ growth rate was enhanced in the low temperature range (<550 °C) and the activation energy was reduced to 1.5 eV for GeH$_4$ = 1.5 sccm. The decrease in activation energy with the addition of a small fraction of GeH$_4$ is consistent with work on Si$_{1-x}$Ge$_x$ epitaxy.[18] This phenomenon was also observed by the LPCVD system,[8] and we speculate that Ge atoms at the growth interface serve as hydrogen desorption centers and reduce the activation energy for hydrogen desorption.[22] As the deposition temperature increases, the curves show lower apparent activation energy less than 0.25 eV. This indicates that the deposition changes from the reaction-rate limited regime to the mass-transport limited regime. Since the chemical surface reaction rate increases rapidly with the addition of GeH$_4$, the reactant gas supply reaching the substrate surface cannot keep up with the demand of the reaction. Therefore, the transition temperature between the reaction-rate limited regime and mass-transport limited regime decreases with increasing GeH$_4$ fraction in the reaction gas.

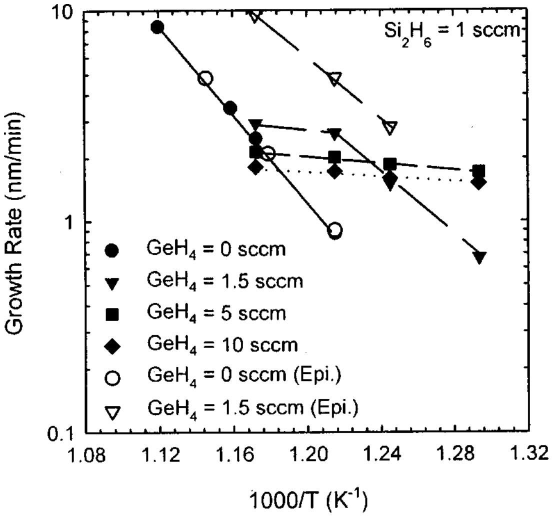

FIG. 4. Film deposition rate as a function of the inverse of deposition temperature for various GeH$_4$ flow rates.

The XRD spectra of the poly-Si$_{1-x}$Ge$_x$ with $x = 0.08$, 0.21, and 0.36 are shown in Fig. 5. Peaks corresponding to the (111), (220), and (311) planes are indicators of diamond crystal structure. All the films show preferential orientation of the (111) plane in spite of Ge fraction. The full width at the half maximum of the XRD peak for the (111) plane is around 0.3°, indicating that the crystallinity of film is good enough compared with typical poly-Si film deposited by LPCVD. The locations of the singular peaks are located in between those of poly-Si and poly-Ge, and are shifted more toward those of pure Ge for the films with higher Ge fraction. The increase in the Ge fraction results in an increase in the lattice constant. The lattice constant was determined by the average of the lattice constants obtained from the (111) and (220) peaks. The lattice constants were used to calculate

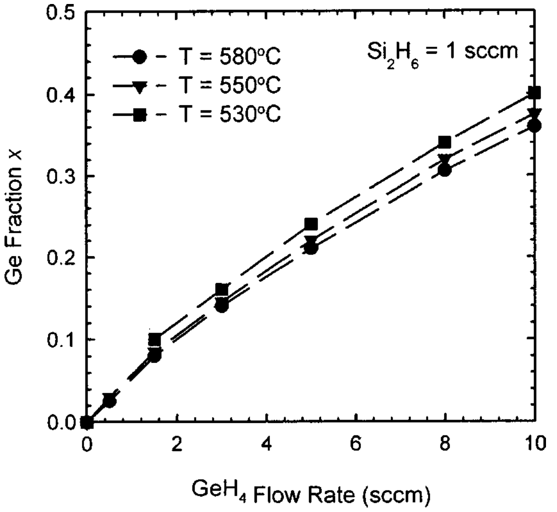

FIG. 6. Dependence of Ge fraction on GeH$_4$ flow rate with Si$_2$H$_6$=1 sccm at different growth temperatures.

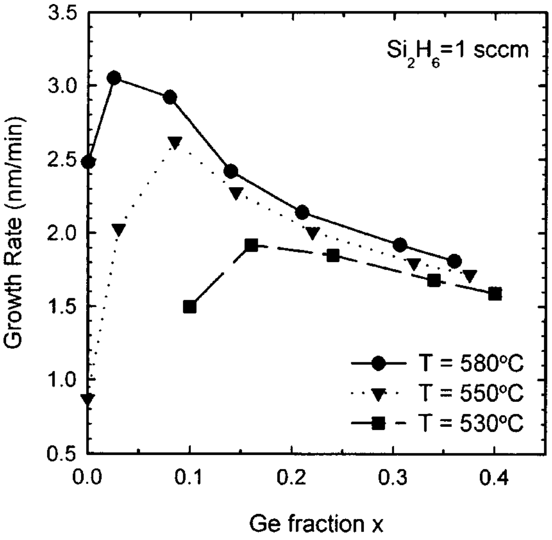

FIG. 7. Growth rates of poly-Si$_{1-x}$Ge$_x$ films as a function of Ge fraction x at different growth temperatures.

the Ge atomic fraction x by Vegard's law. Because the strain of grain is present in the as-deposited poly-Si$_{1-x}$Ge$_x$ films, the lattice distortion exists and affects the precision of measurement. To obtain the measurement uncertainty of the XRD method, some samples were measured by AES. The AES data have been calibrated with Si and Ge standards. Compared with AES analyses, the accuracy of the Ge fraction determined by XRD is within 2 at. %. Figure 6 shows the dependence of the Ge fraction x on the GeH$_4$ flow rate. The Si$_2$H$_6$ flow rate was kept at 1 sccm. The Ge fraction increased monotonically with the increase of the GeH$_4$ flow when the growth temperature remained constant. The Ge fraction increases slightly with the decrease of growth temperature for fixed Si$_2$H$_6$ and GeH$_4$ flow rates. This observation is consistent with previous findings of lower activation energies for germanium deposition compared to those for silicon deposition.[23]

Poly-Si$_{1-x}$Ge$_x$ deposition rate is plotted as a function of the Ge atomic fraction in Fig. 7. Each line represents a constant deposition temperature. The growth rate increases with the Ge fraction at lower values and then decreases with the Ge fraction in the higher composition range. The variation of the deposition rate for poly- Si$_{1-x}$Ge$_x$ films with Ge fraction is significantly different from that of epitaxial ones.[19] This phenomenon was also observed by other UHVCVD system and was explained by the different strain energy contained in the poly- Si$_{1-x}$Ge$_x$ and epitaxial Si$_{1-x}$Ge$_x$.[13] To obtain further insight into the above results, we divided the Si$_{1-x}$Ge$_x$ growth rate R_{SiGe} into the Si growth rate R_{Si} and Ge growth rate R_{Ge}, that is, R_{SiGe} is equal to $(R_{\mathrm{Si}}+R_{\mathrm{Ge}})$. The separation was based on the determined Si and Ge fractions in the Si$_{1-x}$Ge$_x$ films. Figure 8(a) and 8(b) show the Si and Ge growth rates as a function of Ge fraction in the deposited poly-Si$_{1-x}$Ge$_x$ film. For the Si growth rate, a maximum is observed for each temperature. The Si growth rate increases first, and then decreases with Ge fraction. The Ge growth rate, on the other hand, shows no maximum and increases with the Ge fraction in the Si$_{1-x}$Ge$_x$ film. As observed from Fig. 4, the deposition is limited by surface reaction at lower Ge fraction. In this case, R_{Si} depends on the Si$_2$H$_6$ flow rates, surface reaction rate constants, and the hydrogen desorption rate. Hence the initial increase of R_{Si} at lower Ge fraction is caused by enhancement of hydrogen desorption with Ge incorporation. When R_{Si} was increased to a maximum value, R_{Si} began to decrease with increasing Ge fraction. In the higher composition range, the growth rate is not sensitive to the substrate temperature as illustrated in Fig. 4; this indicates that the deposition is controlled by mass transfer. In the mass-transport limited regime, the R_{Si} depends on Si$_2$H$_6$ concentration, and sticking probability of Si$_2$H$_6$ on the Si$_{1-x}$Ge$_x$ surface. Kim *et al.*[24] proposed a model based on the sticking probability of Si and Ge precursors to explain the behavior. They concluded that the decrease of growth rate with increasing Ge content in the mass-transport limited regime is due to the sticking probabilities of both Si and Ge precursors being lower on Ge than on Si. In our UHVCME system, we found that the total growth pressure increases linearly with the increase of GeH$_4$ flow rate due to the constant pump speed as shown in Fig. 9. The increase of the growth pressure will decrease the gas velocity, and hence the Si$_2$H$_6$ concentration reaching the Si$_{1-x}$Ge$_x$ surface. This may also be the reason for the decrease of Si growth rate. However, the actual growth mechanism is not very clear in our UHVCME system, and will be studied in detail in the future. In Fig. 8(a), the peaks shift to the left as the deposition temperature increases. This is simply because the reaction rate increases quickly with the deposition temperature, and the deposition enters the mass-transport limited regime at lower Ge fraction. In Fig. 8(b), R_{Ge} increases monotonically with the Ge fraction and almost does not depend on growth temperature. The increase of R_{Ge} with Ge fraction is mainly due to the increase of the GeH$_4$ concentration in the bulk gas.

For poly-Si$_{1-x}$Ge$_x$ gated MOSFET application, the surface roughness and thickness uniformity of poly-Si$_{1-x}$Ge$_x$

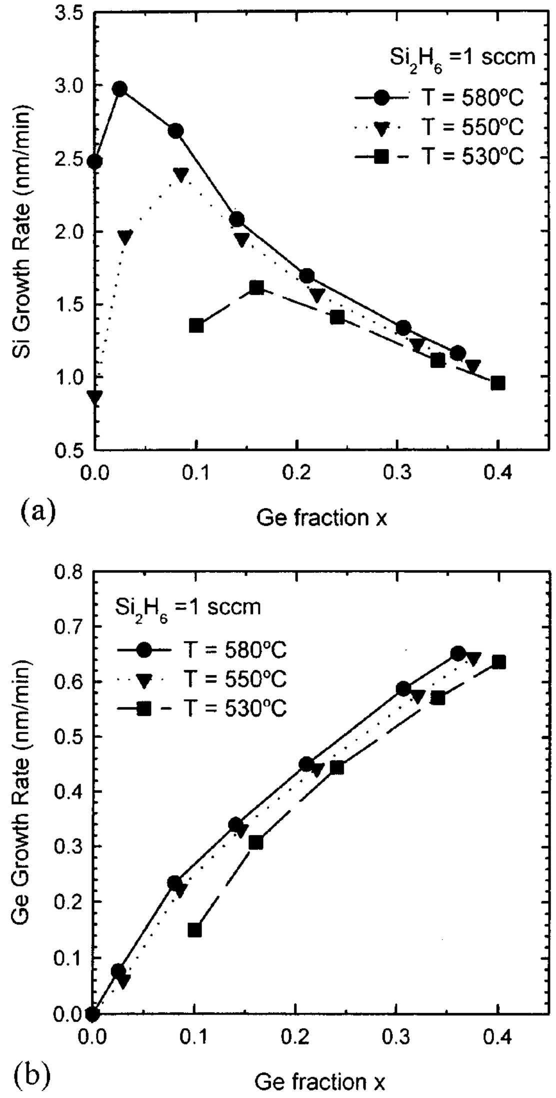

FIG. 8. (a) Si and (b) Ge components of poly-Si$_{1-x}$Ge$_x$ deposition rate vs Ge fraction x at different growth temperatures.

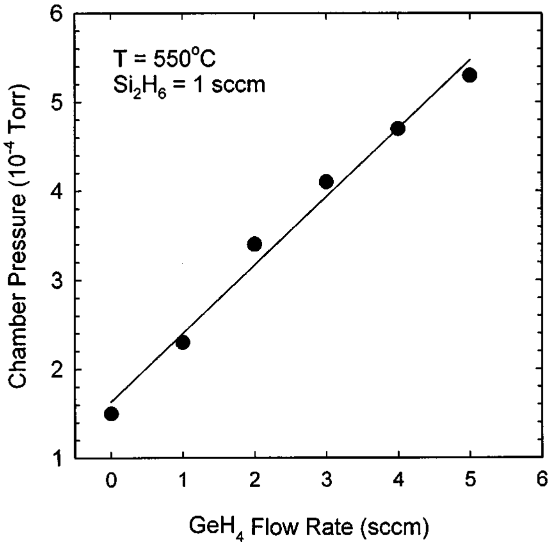

FIG. 9. Growth chamber pressures of the UHVCME system as a function of the GeH$_4$ flow rate during poly-Si$_{1-x}$Ge$_x$ deposition.

with nitride substrate were investigated. The maximum peak-to-peak surface roughness and thickness uniformity of poly-Si$_{1-x}$Ge$_x$ films grown on nitride at 580 and 550 °C are shown in Table I. The surface roughness of poly-Si$_{1-x}$Ge$_x$ films increases as the GeH$_4$ flow rate increased at the same temperature. This is probably because the grain size of polycrystals becomes larger when the Ge fraction increased. The average grain size was estimated to be 150–180 nm for poly-Si$_{0.79}$Ge$_{0.21}$ deposited at 580 °C by SEM measurements. In addition, the smoother films are obtained by lowering the deposition temperature. The thickness uniformity of poly-Si is 16% at 580 °C, and it is undesirable for device application. As observed in Fig. 4, the deposition of poly-Si is limited by surface reaction, so the growth rate of films is strongly dependent on the growth temperature. Because the temperature distribution of the substrate heater is not constant, the film thickness is not uniform across the wafer. The thickness uniformity of poly-Si$_{1-x}$Ge$_x$ films can be improved by the addition of germanium. As illustrated in Table I, the uniformity is 2.5% for GeH$_4$ = 1.5 sccm, and reduces to 1.9% for GeH$_4$ = 10 sccm at 580 °C. The deposition of poly-Si$_{1-x}$Ge$_x$ is limited by mass transfer at 580 and 550 °C. The growth rate tends to become temperature insensitive. For the UHVCME reactor, an equal flux of reactants to all locations of a wafer surface is supplied, so the thickness uniformity can be improved in the mass-transport limited regime.

IV. CONCLUSIONS

Si$_2$H$_6$ and GeH$_4$ are used to grow poly-Si$_{1-x}$Ge$_x$ by the cold-wall UHVCME process. The Ge fraction and growth rate of poly-Si$_{1-x}$Ge$_x$ were found to be dependent on the GeH$_4$ flow rate at a constant Si$_2$H$_6$ flow, while not on the substrate type. The Ge fraction increased monotonically with the increase of GeH$_4$ flow. The Si$_{1-x}$Ge$_x$ growth rates for various Ge fractions were separated into Si growth rate and Ge growth rate. From the results obtained, Si growth rate is greatly enhanced by introduction of a small amount of GeH$_4$, and then decreases when the Ge fraction is further increased. The decrease of growth rate is due to the reduction of the Si$_2$H$_6$ concentration or the sticking probabilities of precursors on the Si$_{1-x}$Ge$_x$ surface in mass-transport limited regime. Besides the above effects in Si growth rate, Ge growth

TABLE I. Thickness uniformity and surface roughness of poly-Si$_{1-x}$Ge$_x$ films at 550 and 580 °C with nitride substrate. The Si$_2$H$_6$ flow rate remained at 1 sccm.

	T = 550 °C		T = 580 °C	
GeH$_4$ (sccm)	Roughness (%)	Uniformity (%)	Roughness (%)	Uniformity (%)
0	5.6	14	8.2	16
1.5	9.1	2.6	11	2.5
5	10	2.2	13	2.1
10	11	1.7	15	1.9

rate shows a strong dependence on the GeH_4 flow rate. Therefore, the relative variations of the hydrogen desorption rate, source gas concentration, and sticking probability of precursor under different growth conditions are used to explain the above results consistently in this study. The thickness uniformity of poly-$Si_{1-x}Ge_x$ films depends on the Ge fraction, and it is improved by the addition of germanium. The result can be explained by the lower activation energy related to deposition of poly-$Si_{1-x}Ge_x$ in the mass-transport regime. In this regime, the Ge fraction and growth rate of poly-$Si_{1-x}Ge_x$ are well controlled.

ACKNOWLEDGMENTS

The authors would like to thank Dr. H. C. Lin and C. Y. Lin for experimental assistance. This work was supported by the Republic of China's National Science Council through Contract No. NSC88-2215-E009-048.

[1] T.-J. King and K. C. Saraswat, Tech. Dig. Int. Electron Devices Meet. 567 (1991).
[2] T.-J. King, J. R. Pfiester, J. D. Shott, J. P. MccVittie, and K. C. Saraswat, Tech. Dig. Int. Electron Devices Meet. 253 (1990).
[3] P.-E. Hellberg, S.-L. Zhang, and C. S. Petersson, IEEE Electron Device Lett. **18**, 456 (1997).
[4] Y. V. Ponomarev, C. Salm, J. Schmitz, P. H. Woerlee, P. A. Stolk, and D. J. Gravesteijn, Tech. Dig. Int. Electron Devices Meet. 829 (1997).
[5] W. C. Lee, T.-J. King, and C. Hu, IEEE Electron Device Lett. **20**, 9 (1999).
[6] J. Holleman, A. E. T. Kuiper, and J. V. Verweij, J. Electrochem. Soc. **140**, 1717 (1993).
[7] T.-J. King and K. C. Saraswat, J. Electrochem. Soc. **141**, 2235 (1994).
[8] M. Cao, A. Wang, and K. C. Saraswat, J. Electrochem. Soc. **142**, 1566 (1995).
[9] N. Kistler and J. Woo, Tech. Dig. Int. Electron Devices Meet. 727 (1993).
[10] M. Sanganeria, D. T. Grider, M. C. Ozturk, and J. J. Wortman, J. Electron. Mater. **21**, 614 (1992).
[11] K. Shiota, D. Inoue, K. Minami, M. Yamamoto, and J. Hanna, Jpn. J. Appl. Phys., Part 2 **36**, L989 (1997).
[12] H. C. Lin, T. G. Jung, H. Y. Lin, C. Y. Chang, T. F. Lei, P. J. Wang, R. C. Deng, J. Lin, and C. Y. Chao, J. Appl. Phys. **74**, 5395 (1993).
[13] H. C. Lin, C. Y. Chang, W. H. Chen, W. C. Tsai, T. C. Chang, T. G. Jung, and H. Y. Lin, J. Electrochem. Soc. **141**, 2559 (1994).
[14] A. T. Voultsas and M. K. Hatalis, J. Electrochem. Soc. **139**, 2659 (1992).
[15] D. Meakin, J. Stoemenus, P. Migliorato, and N. A. Economou, J. Appl. Phys. **61**, 5031 (1987).
[16] M. Miyasaka, T. Nakanaza, I. Yudasaka, and H. Ohshima, Jpn. J. Appl. Phys., Part 1 **30**, 3733 (1991).
[17] H. C. Lin, H. Y. Lin, C. Y. Chang, T. F. Lei, P. J. Wang, and C. Y. Chao, Appl. Phys. Lett. **63**, 1351 (1993).
[18] G. W. Huang, L. P. Chen, C. T. Chou, K. M. Chen, H. C. Tseng, W. C. Tsai, and C. Y. Chang, J. Appl. Phys. **81**, 205 (1997).
[19] L. P. Chen, C. T. Chou, G. W. Huang, W. C. Tsai, and C. Y. Chang, Appl. Phys. Lett. **67**, 3001 (1996).
[20] J. T. Fitch, J. Electrochem. Soc. **141**, 1046 (1994).
[21] K. Sinniah, M. G. Sherman, L. B. Lewis, W. H. Weinberg, J. T. Yates, and K. C. Janda, Phys. Rev. Lett. **62**, 567 (1989).
[22] M. Stutzmann, R. A. Street, C. C. Tsai, J. B. Boyce, and S. E. Reach, J. Appl. Phys. **66**, 569 (1989).
[23] T. I. Kamina and D. J. Meyer, Appl. Phys. Lett. **59**, 178 (1991).
[24] H. Kim, N. Taylor, T. R. Bramblett, and J. E. Greene, J. Appl. Phys. **84**, 6372 (1998).